ESTIMATION OF ELECTRIC FIELD FLUCTUATIONS BELOW THE AURORAL IONOSPHERE

Takasi OGUTI and Kanji HAYASHI

Geophysics Research Laboratory, University of Tokyo, 3-1, Hongo 7-chome, Bunkyo-ku, Tokyo 113

Abstract: A fluctuation in an electric field below a pulsating aurora, as well as an electric field intensity below a discrete aurora (vortex-chain aurora), or an auroral ionosphere where an electric field is applied from the magnetospheric convection, was estimated at a 30 km altitude (possible balloon altitude) and on the ground by a theoretical model. The results show that the electric field fluctuation, corresponding to an auroral pulsation, is usually as small as a few percents and a few tens of percent, respectively, of the ionospheric electric field when measured at a 30 km altitude and on the ground when the size of the pulsating auroral patch is 50 km across. On the other hand, the electric field below the ionospheric, related to a discrete aurora or convection electric field above, is shown to amount to the value almost equal to, and 20 times larger than, the ionospheric value respectively at the 30 km altitude and on the ground, if a north-south, uniform or convergent electric field exists in an east-west elongated belt, 200 km in width, in the ionosphere. It is also shown that the values of the electric field and its fluctuation both at the 30 km altitude and on the ground depend largely on the size of the spatial extent of the electric field in and above the ionosphere. These results suggest that the electric field fluctuation related to the auroral pulsation is measured only by the multiple correlation method taking the all auroral patches within range into consideration even when the size of auroral patch is greater than tens of km. The calculation also suggests that the electric field related to a discrete aurora or the convection electric field could be measured by taking a spatial correlation and/or multiple correlations with auroral variations of electric field fluctuations obtained at ground network stations below the auroral ionosphere.

1. Introduction

In the previous studies (OGUTI *et al.*, 1984; OGUTI and HAYASHI, 1984), we showed that the magnetic pulsations on the ground below a pulsating aurora are fully explained by electric currents. These currents are theoretically expected to be induced in a local enhancement of conductivity caused by pulsating precipitation of auroral electrons, in conjunction with the convection electric field inferred from auroral drifts. Since the agreement between observation and calculation of the fluctuation magnetic field on the ground was perfect in the previous result (OGUTI and HAYASHI, 1984), the estimated electric currents must represent the real currents. The estimated electric field in the calculation is also concluded to be a good approximation of what really takes place in and around the pulsating auroral form. In this paper, fluctuation electric field intensities below a pulsating aurora are first examined on the basis of the

ionospheric electric field obtained in the previous paper (OGUTI and HAYASHI, 1984). Also in this paper electric field intensities below a discrete (vortex-chain) aurora or below an auroral ionosphere where the convection electric field is applied from the magnetosphere are estimated, for testing the possibility of monitoring the ionospheric electric field and its fluctuations on the ground.

2. Electric Field Fluctuation below a Pulsating Aurora

In calculating the electric field and the electric current around an auroral patch in the previous study, an electric potential in and above the ionosphere is expressed, using ordinary polar coordinates, r and θ, as

$$\begin{aligned} \phi^{\mathrm{o}} &= (r\cdot E + C/r)\cdot\cos\theta + (D/r)\cdot\sin\theta \\ \phi^{\mathrm{i}} &= (E+C)\cdot r\cdot\cos\theta + D\cdot r\cdot\sin\theta \ . \end{aligned} \tag{1}$$

In this expression, E is the ambient electric field, and C and D are given by

$$C = -\frac{-\{(\Sigma_2^{\mathrm{i}}-\Sigma_2^{\mathrm{o}})^2+(\Sigma_1^{\mathrm{i}}-\Sigma_1^{\mathrm{o}})(2M+\Sigma_1^{\mathrm{i}}+\Sigma_1^{\mathrm{o}})\}E}{(\Sigma_2^{\mathrm{i}}-\Sigma_2^{\mathrm{o}})^2+(2M+\Sigma_1^{\mathrm{i}}+\Sigma_1^{\mathrm{o}})^2} \ , \tag{2}$$

$$D = \frac{-2(\Sigma_2^{\mathrm{i}}-\Sigma_2^{\mathrm{o}})(M+\Sigma_1^{\mathrm{o}})E}{(\Sigma_2^{\mathrm{i}}-\Sigma_1^{\mathrm{o}})^2+(2M+\Sigma_1^{\mathrm{i}}+\Sigma_1^{\mathrm{o}})^2} \ , \tag{3}$$

and

$$M = \frac{\Sigma_1^{\mathrm{o}}+\Sigma_1^{\mathrm{i}}}{2}\cdot\frac{P}{100-P} \ . \tag{4}$$

The superscripts o and i indicate the outside and inside of the domain, Σ_1^{o} and Σ_1^{i} are height-integrated Pedersen conductivities outside and inside the domain respectively, and P is the field-aligned discharge rate, defined as a percentage of the field-aligned component to the total discharge rate (field-aligned discharge plus ionospheric discharge).

These results were based on various assumptions: the ionosphere is a thin sheet, the ambient magnetic field is vertical, the conductivity enhancement is uniform in the auroral patch, the patch is circular and the field-aligned discharge current is limited to the field lines passing through the patch boundary.

Then the electric field and the electric currents were calculated by

$$\vec{E}_\perp = -\mathrm{grad}_\perp\phi; \quad \vec{J}_\perp = (\Sigma)\cdot\vec{E}_\perp; \quad \vec{J}_\parallel = \mathrm{div}_\perp\vec{J}_\perp \ , \tag{5}$$

using the Hall/Pedersen conductivity ratio, conductivity enhancement factor, and field-aligned discharge rate as parameters.

An example of the calculation of electric currents and electric field in and around the domain is reproduced from the previous paper (OGUTI and HAYASHI, 1984) in Figs. 1a to 1e for the convenience of the reader. Figure 1a shows a total electric current including the ambient (jet) current, while Fig. 1b is an additional current due to conductivity enhancement of the domain, obtained by subtracting the uniform ambient current from the total current in Fig. 1a. The additional current in Fig. 1b is divided into

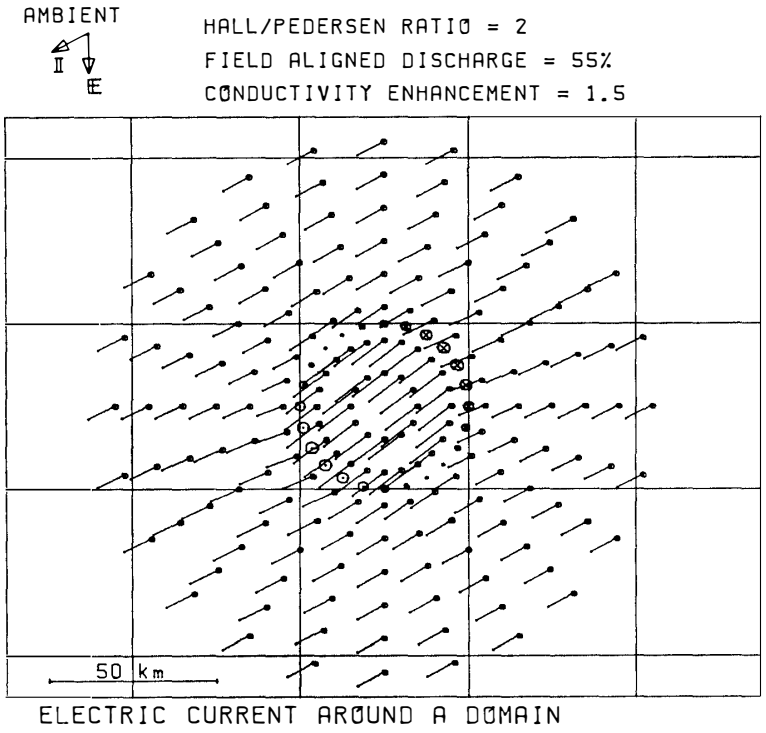

Fig. 1a. The total current including the uniform, ambient current.

Figs. 1a–e. An example of the electric current calculated in the vicinity of a conductivity enhancement domain.

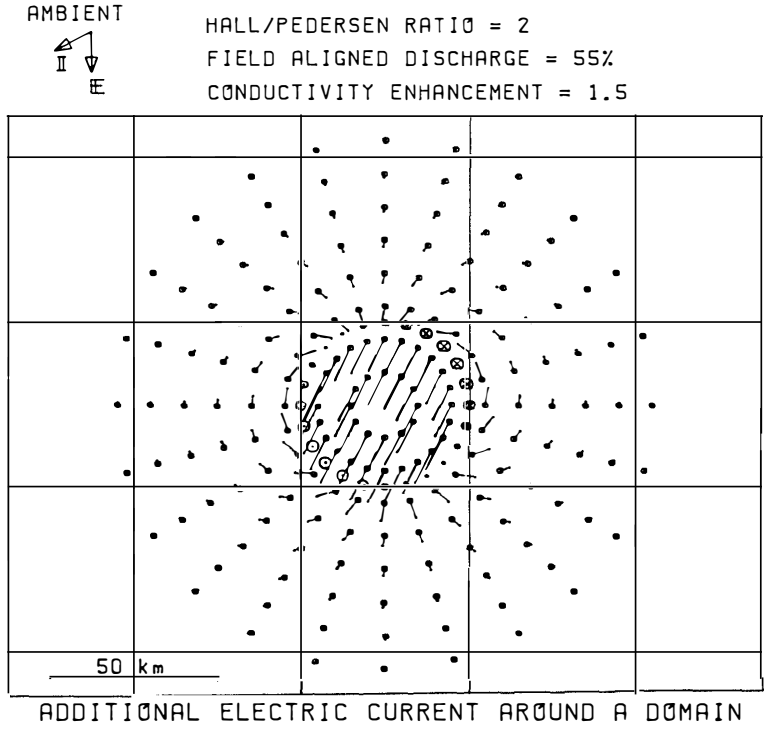

Fig. 1b. Additional electric current induced in the vicinity of the conductivity enhancement region.

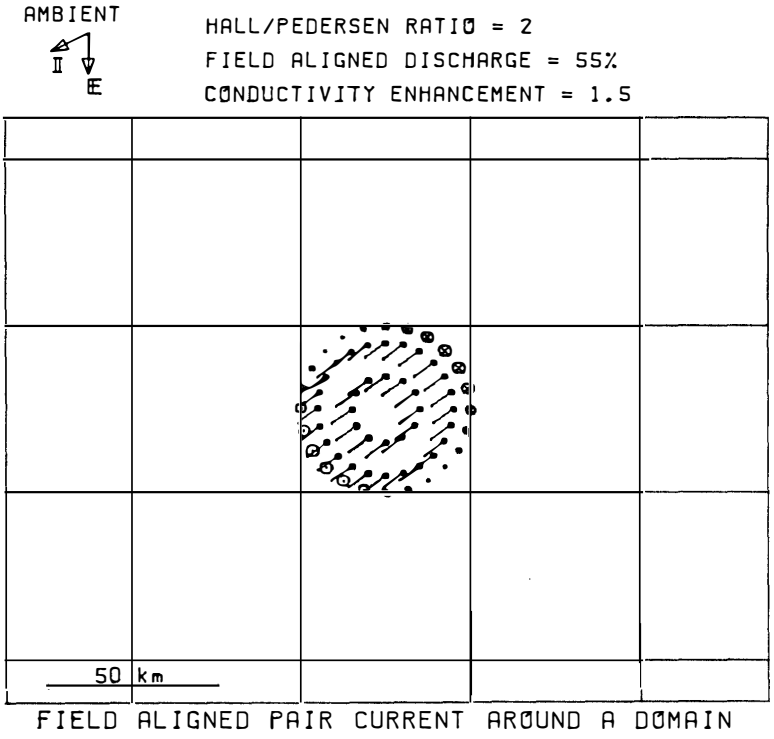

Fig. 1c. A field-aligned pair current, connected in the conductivity enhancement region.

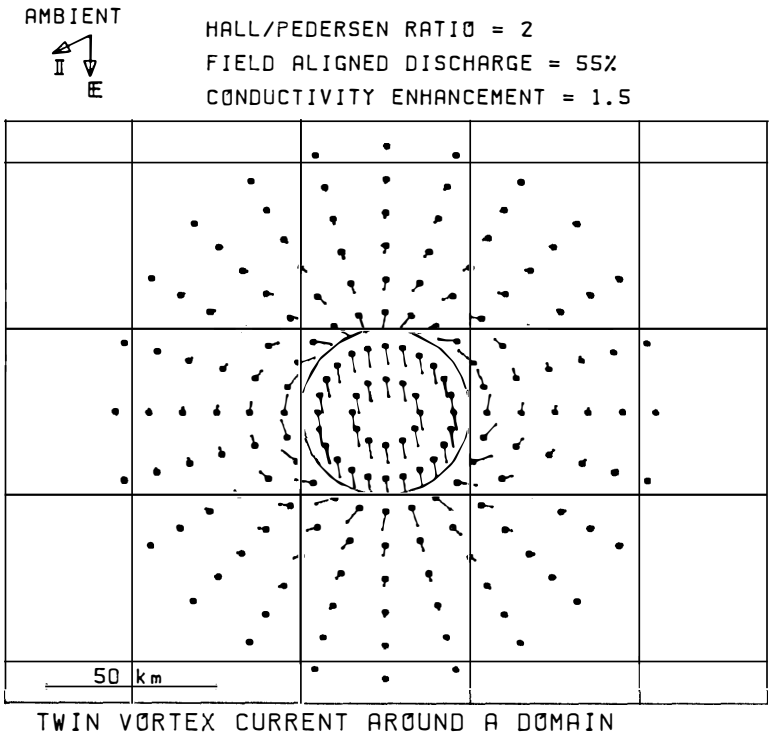

Fig. 1d. A twin-vortex current which is connected inside with the outside part of the additional current in Fig. 1b without divergence at the boundary.

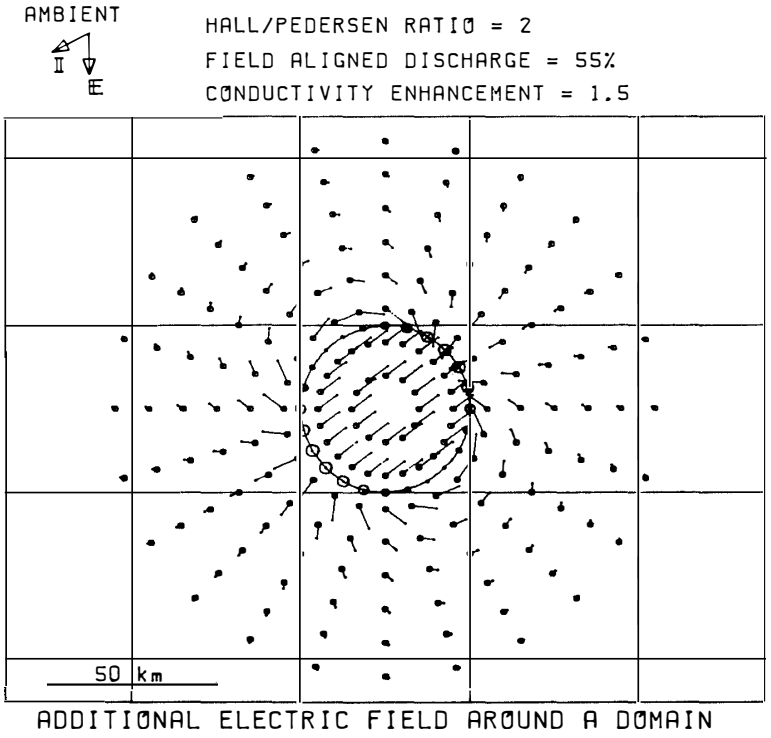

Fig. 1e. The ionospheric (and higher) electric field related to this current system.

two parts, a field-aligned pair current which is connected in the domain, and a twin-vortex current which closes in the ionosphere connected inside to the outer part of the additional current in Fig. 1b without divergence at the boundary. Figure 1c indicates the field-aligned pair current and Fig. 1d the twin-vortex current, thus separated.

Figure 1e illustrates an additional electric field which is produced by the space charge at the domain boundary and contributes to the fluctuation of the electric field around the pulsating auroral patch. In contrast to the magnetospheric dynamo, the electromotive force here is produced by the local conductivity enhancement in the ionosphere. That is, the ionospheric current which is directly connected to the field-aligned pair current is the source of the charge separation in the domain. Therefore, the electric field is reversed to the ionospheric part of the field-aligned pair current inside the domain, and it extends outside in the ordinary two dimensional form, as shown in Fig. 1e. Although a similar calculation of electric current around a local enhancement of conductivity in the ionosphere was carried out by STUBBE and KOPKA (1977) in relation to ionospheric modification experiments, they neglected field-aligned discharge at the boundary so that the field-aligned pair current is missing in their result. The calculation of Figs. 1a to 1e is based on a Hall/Pedersen conductivity ratio of 2, conductivity enhancement factor of the domain of 1.5, and field-aligned discharge rate of 55%. The 55% field-aligned discharge rate was obtained by comparing the calculation with the observation of magnetic variations.

An important scope of the calculation is that it predicts the pattern and the intensity of the electric field which is additionally produced around and below the pulsating auroral patches as the auroral patch pulsates. Two examples of calculation of the

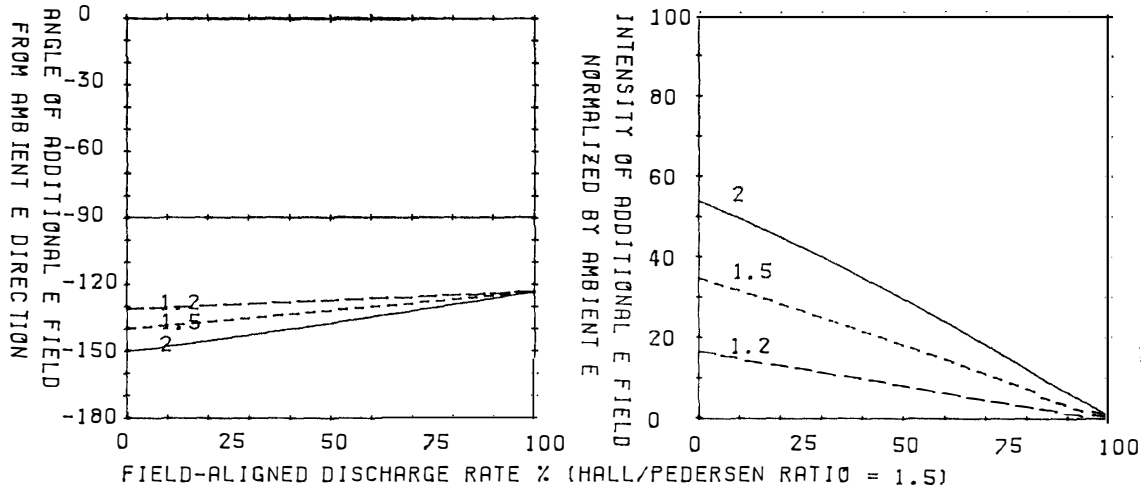

(*a*) *Hall/Pedersen ratio of 1.5.*

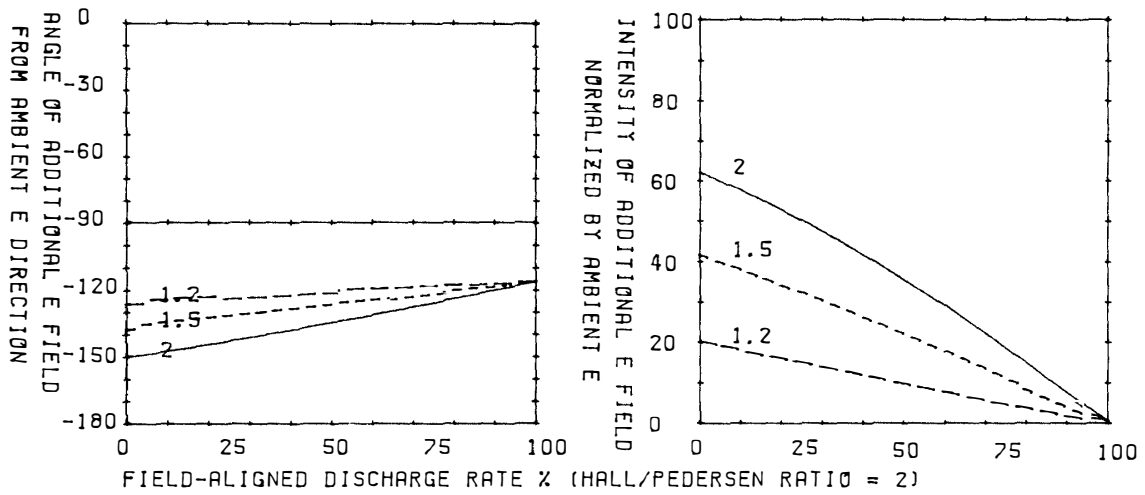

(*b*) *Hall/Pedersen ratio of 2.*

Figs. 2a, b. The calculated changes in direction (left) and intensity (right) of the additional electric field in a domain versus the field-aligned discharge rate. The direction is given in an angle from the ambient electric field, and the intensity is normalized by the ambient field intensity.

intensities and directions of the additional electric field in and above the ionosphere are also reproduced in Figs. 2a and 2b. As shown in Fig. 2a and 2b, postulating 55% field-aligned discharge, the intensity of the additional electric field in the domain is about 20% of the ambient (convection) electric field in the case of 1.5 times conductivity enhancement and it is about 10% in the case of 1.2 times enhancement.

The additional electric field extends below the ionosphere as shown by PARK (1976), and may be observed by balloon below pulsating auroras. Distribution of the fluctuation electric fields below a pulsating aurora is estimated by extending the electric field in Fig. 1e below the ionosphere using Fourier-Bessel expansions. If we assume that the conductivity is isotropic and exponentially decreases as $\exp(-\alpha z)$

(downward positive for z) with decrease in altitude below the ionosphere, the electric potential, ϕ, must satisfy the relation as

$$\partial^2\phi/\partial x^2+\partial^2\phi/\partial y^2+\partial^2\phi/\partial z^2-\alpha\partial\phi/\partial z=0\,, \tag{6}$$

due to the source-free condition of the current, $\mathrm{div}\,\vec{J}=0$. The solution of this equation is, using ordinary polar coordinates, r, θ and z, given as

$$\begin{aligned}\phi=&\sum_k\sum_n J_n(kr)\sin(n\theta)[A_n^k\exp\{\alpha-(\alpha^2+4k^2)^{1/2}\}z/2+B_n^k\exp\{\alpha+(\alpha^2+4k^2)^{1/2}\}z/2]\\&+\sum_k\sum_n J_n(kr)\cos(n\theta)[C_n^k\exp\{\alpha-(\alpha^2+4k^2)^{1/2}\}z/2+D_n^k\\&\times\exp\{\alpha+(\alpha^2+4k^2)^{1/2}\}z/2]\,,\end{aligned} \tag{7}$$

where the coefficients A_n^k, B_n^k, C_n^k and D_n^k are determined by the ionospheric and ground boundary conditions; that is, the continuity of the electric potential at the ionospheric boundary, and the equipotential at the ground surface. Note that the attenuation of the electric field with distance, z, is much reduced by the steep decrease in electric conductivity below the ionosphere. As seen in eq. (7), the electric field intensity would decrease as $\exp(-kz)$ with decrease in altitude in the vacuum or in the uniform conductivity region, where $\alpha=0$, while the decreasing rate in this case is reduced to $\exp\times[\alpha-(\alpha^2+4k^2)^{1/2}]z/2$. This is an essential factor which allows the small scale electric field, such as is due to pulsating aurora, to penetrate well down to the lower altitudes as shown below.

An estimate of the fluctuation electric field below a brightened auroral domain is shown in Figs. 3 and 4. Figure 3 represents the distribution of fluctuation electric field in a vertical section, which includes the symmetry axis of the additional electric field, and Fig. 4 shows the electric field distribution at a possible balloon altitude of 30 km, both on the basis of the parameters, Hall/Pedersen conductivity ratio of 2, conductivity enhancement factor of 1.5 and field-aligned discharge rate of 55%. In calculation, it is assumed that the atmospheric conductivity below the ionosphere decreases one order of magnitude with every 10 km decrease in altitude. It is seen in

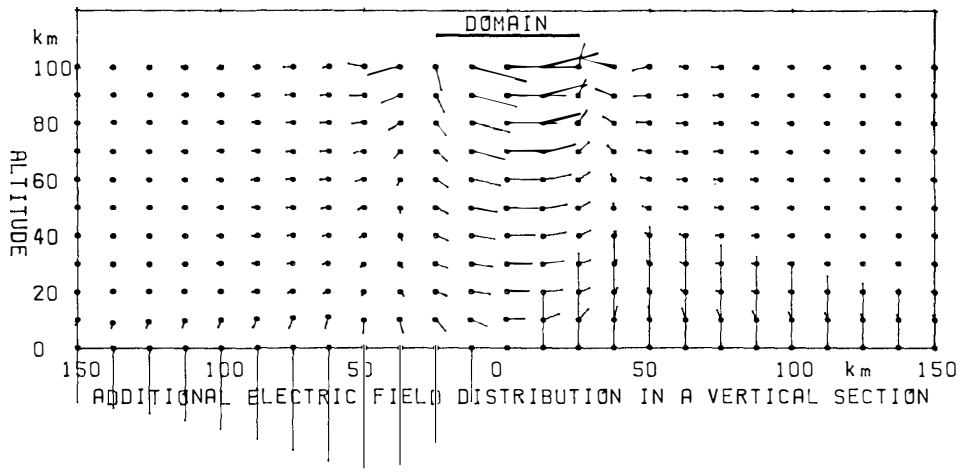

Fig. 3. Distribution of estimated fluctuation electric field below a brightened domain in a vertical section including symmetry axis of the additional electric field.

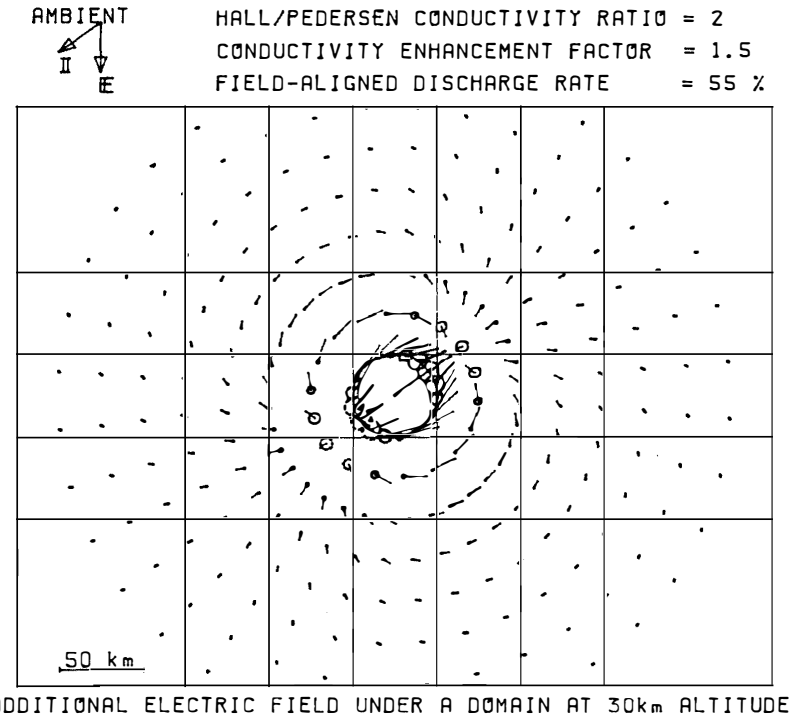

Fig. 4. Distribution of fluctuation electric field at a 30 km altitude. Vertical intensities are given by circles (solid upward, dashed downward) and horizontal components are given by arrows from the center circles. Note that both the divergence and the convergence are about 40 km from the center of the brightened auroral domain.

Fig. 3 that the fluctuation intensity at the 30 km altitude under a pulsating domain is approximately 35% of the additional electric field in the domain. This, together with the results in Figs. 2a and 2b, indicates that the fluctuation electric field intensity related to a pulsating patch, when measured just under the domain, is about 7% of the convection electric field in the case of 1.5 times conductivity enhancement. This reduces to 3.5% in the case of 1.2 times enhancement.

Although we used a 50 km scale size of the patch in the calculation corresponding to the 50 km grid size in the analysis in the previous study (OGUTI and HAYASHI, 1984), actual patch size is usually smaller so that the field also tends to be smaller and, hence, the measurement of the fluctuation electric field below a pulsating aurora by a balloon would be quite difficult in terms of the contamination of large atmospheric components. The fluctuation electric field may be detectable at the balloon altitude only when a patch is much larger than the domain size here, 50 km across.

The calculation predicts the distribution pattern of the fluctuation of electric field (additional electric field) below a pulsating auroral patch as shown in Fig. 4. The electric field fluctuation must show this pattern, if measured at balloon altitude. However, even if it is actually measured, the electric field fluctuation the same as the magnetic deflection in the previous study by OGUTI and HAYASHI (1984), again is the spatial integration of the contributions from various patches. Therefore, only the multiple correlation technique, applied there to the analysis of the magnetic field, can deduce the electric field contributions from various patches. Note that the divergence and the

convergence in Fig. 4 are only about 40 km from the center of the brightened domain in contrast to the 120 km distances of those in the ground magnetic deflection patterns in the previous result. The difference is due partially to the difference in altitude, but more essentially to the conductivity distribution below the ionosphere as seen in Fig. 3.

It is worth noting in Fig. 3 that the vertical component of the fluctuation electric filed at the ground surface is about 4 times larger than the horizontal component at the balloon altitude, and amounts to about twice that in the auroral patch, due to the space charge effect at the ground surface.

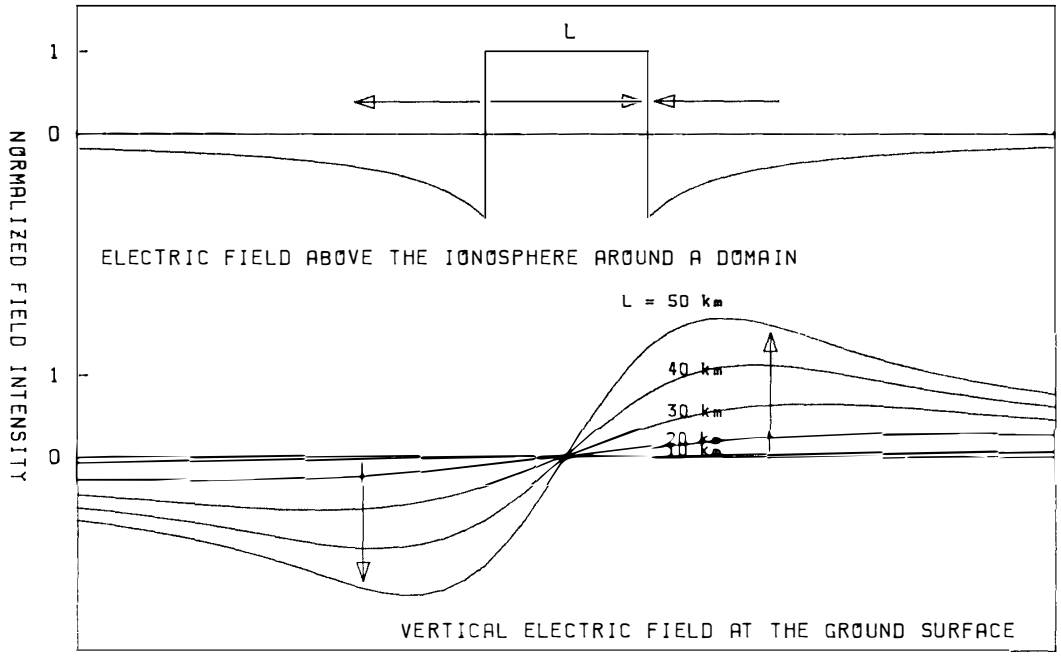

Fig. 5. Spatial distribution of the vertical electric field intensity expected on the ground below a brightened auroral patch of a pulsating aurora. The ground electric field intensity is found to depend largely on the size of the patch, L.

The intensity of the additional electric field below the ionosphere depends largely on the horizontal size of the patch. An estimation of the scale dependence of the vertical field intensity on the ground is shown in Fig. 5. It is known in this figure that the vertical field intensity rapidly decreases with decrease in the horizontal size, L, of the patch, from a value of about twice that in a patch with a size of 50 km across to a few % of that in a 10 km size patch. The vertical electric field fluctuation on the ground caused by a pulsating auroral patch may thus be measurable only when the patch size is larger than several tens of km.

3. Electric Field associated with a Discrete Auroral Form or the Convection Electric Field

The above consideration can also be applied to a discrete aurora, which is regarded

to be a vortex chain (OGUTI, 1981), or to the ionospheric electric field caused by the magnetospheric convection. Since the vortex-chain nature of a discrete aurora indicates a temporal enhancement of electric field convergent towards the auroral arc, elongated in the east-west direction, the electric field at the ionospheric level here is assumed to be two-dimensionally convergent field. Equation (7) is then modified to a simpler form as

$$\phi=\sum_k \sin(kx)[A_k \exp\{\alpha-(\alpha^2+4k^2)^{1/2}\}z/2+B_k \exp\{\alpha+(\alpha^2+4k^2)^{1/2}\}z/2] + \sum_k \cos(kx)[C_k \exp\{\alpha-(\alpha^2+4k^2)^{1/2}\}z/2+D_k \exp\{\alpha+(\alpha^2+4k^2)^{1/2}\}z/2] , \quad (8)$$

where x is the distance in the north-south direction.

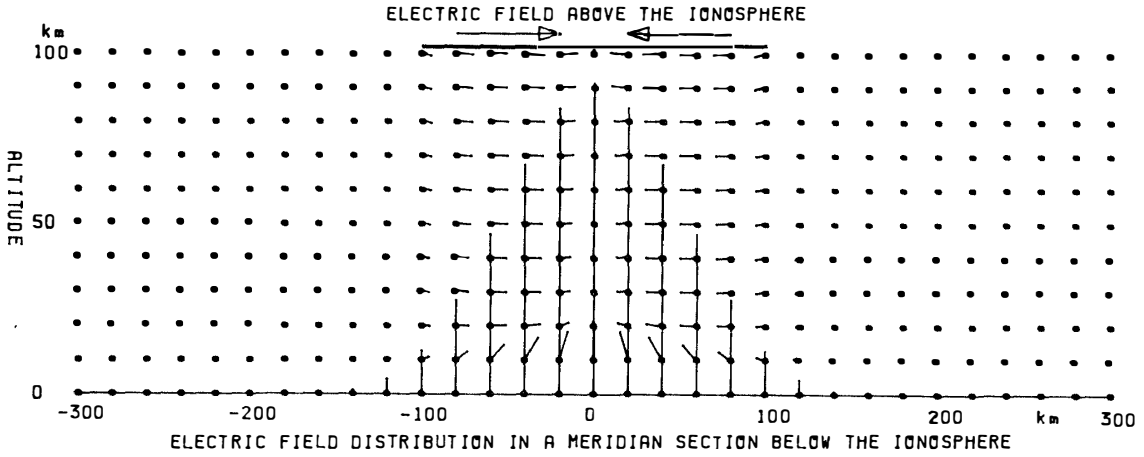

Fig. 6. Electric field distribution below the ionosphere when a two-dimensionally convergent electric field is applied in the north-south direction in and above the ionosphere within an east-west elongated belt, 200 km in width. The upward electric field under the convergence on the ground is found to be about 20 times the horizontal component in the ionosphere.

Assuming again that the electric conductivity below the ionosphere decreases one order of magnitude for every 10 km decrease in altitude, the electric field distribution in a meridian plane is estimated as shown in Fig. 6. Here, it is assumed that a two-dimensionally convergent electric field in the north-south direction exists above the ionosphere within an east-west elongated belt 200 km in width, with a uniform intensity. The electric field intensity at the 30 km altitude is roughly the same as the horizontal field intensity in the ionosphere as seen in the figure. On the other hand, vertical electric field on the ground under the convergence is found to be about 20 times larger than that. The change in the ground electric field intensity with change in the characteristic width, L, is shown in Fig. 7. Again, a strong dependence of the ground field intensity on the scale is evident. It is about 20 times when the width is 200 km, and decreases to roughly the same value as in the ionosphere when the size decreases to 40 km. When the electric field above the ionosphere is not convergent and uniform within a belt, the vertical electric field intensity is found to be modified as shown in Fig. 8, but the scale dependence of the intensity is roughly the same as in the previous case.

These results indicate that the horizontal electric field in the ionosphere with an

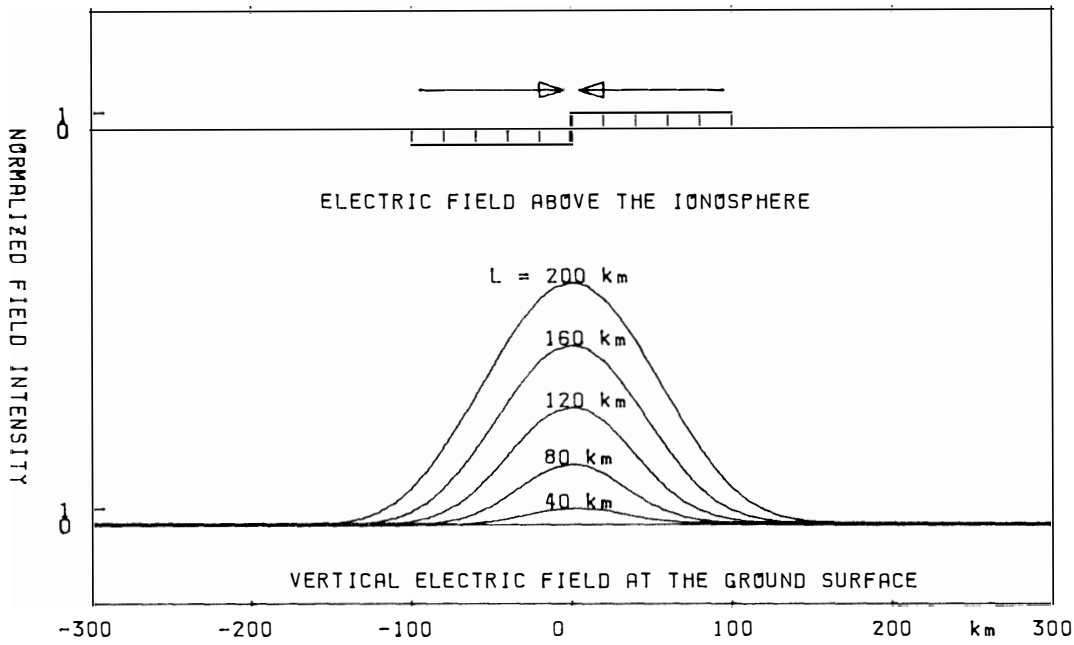

Fig. 7. Spatial distribution of the vertical electric field intensity on the ground below a two-dimensionally convergent ionospheric electric field. The ground electric field is found to be largely dependent on the characteristic scale size of the ionospheric electric field.

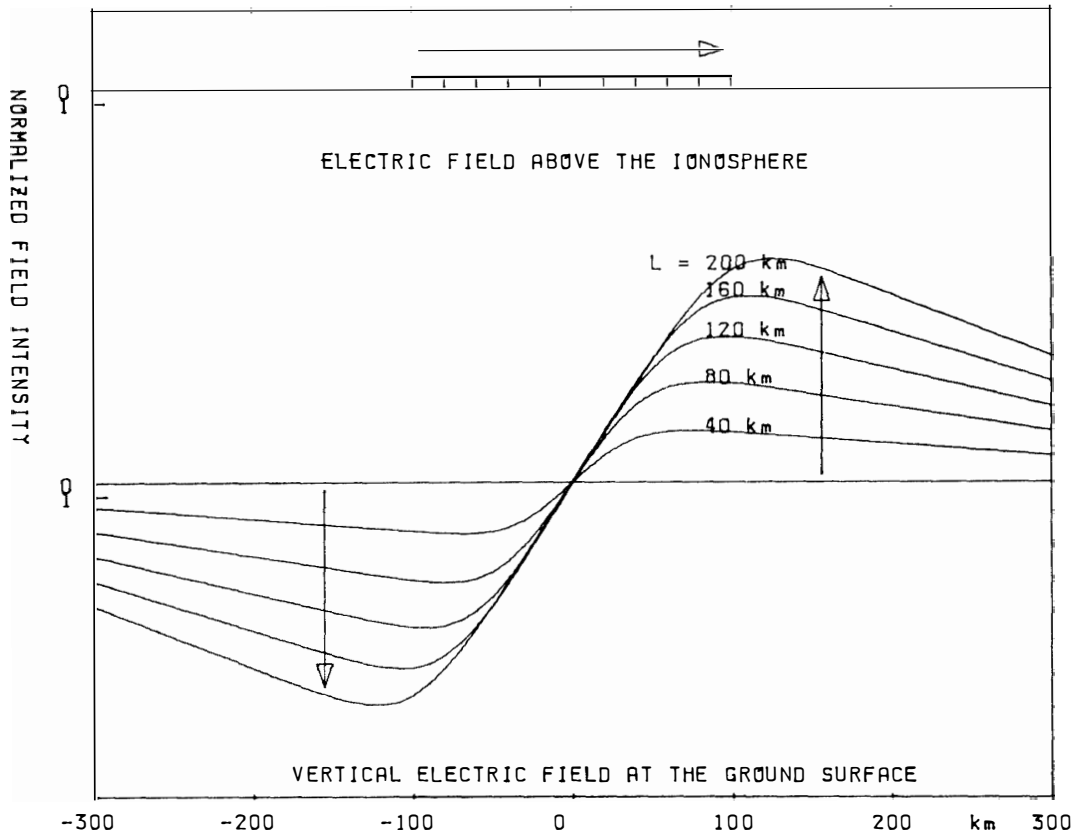

Fig. 8. Spatial distribution of the vertical electric field intensity on the ground below an ionospheric belt where the electric field is uniform. The dependence of the ground field intensity on the characteristic size is similar to that in Fig. 7.

intensity of 50 mV/m causes the vertical electric field on the ground with an intensity of up to 1 V/m when the ionospheric electric field is distributed in a belt with a width as broad as 200 km. Thus, the contribution of the ionospheric electric field to the vertical electric field on the ground is estimated to be about 1% of the background atmospheric electric field near the surface, which usually amounts to 100 V/m on the average.

The 1% contribution of the vertical electric field appears to be fairly difficult to measure if it is stationary because of a possible variability of the background. However, the result also shows how the distribution of the ionospheric contribution should be in relation to the auroral distribution or the configuration of the ionospheric electric field. If the ionospheric electric field varies or moves, the resultant variation in the vertical electric field on the ground must be distributed as shown in Fig. 7 or 8. This suggests that the temporal variations of the vertical electric field synchronous with an auroral brightening or movement appear to be distributed in the same fashion. Therefore, if the vertical electric field components varying synchronously with auroral activity could be separated from the background, and if their spatial distribution could be determined by network observations, the ionospheric electric field distribution could be estimated by comparing it with calculations as Fig. 7 or 8. A spatial correlation of the variation at network stations would also be useful for distinguishing the ionospheric contribution from the vertical electric field on the ground, taking the possible distributions into consideration.

4. Conclusion and Discussion

The possible distribution pattern and the intensity of fluctuation electric field below a pulsating aurora, and a discrete aurora or the auroral ionosphere with the convection electric field were examined in this paper. Conclusion is summarized as follows:

1) The intensity of the fluctuation electric field due to a pulsating auroral patch that is 50 km across will be a few % of the convection electric field, with a pair of divergence and convergence of horizontal field component, both about 40 km from the center of the brightened domain at an altitude of 30 km. The contribution of a pulsating patch to the vertical electric field on the ground is approximately twice the additional electric field in the brightened patch and about a half of the convection electric field.

2) The intensity of horizontal electric field at the 30 km altitude caused by a two-dimensionally convergent electric field in the ionosphere is almost the same as that in the ionosphere, and the ionospheric contribution to the vertical electric field on the ground could amount to 20 times that in the ionosphere, when the ionospheric electric field exists in an ionospheric belt with a width of 200 km. Thus the ionospheric contribution to the field intensity is expected to be 1 V/m on the ground when it is 50 mV/m in the ionosphere.

3) The ionospheric contributions to electric field intensity and its fluctuation below the ionosphere depend largely on the spatial size of the ionospheric electric field. Both could amount to a measurable range when the size of the ionospheric electric field or auroral activity is larger than some tens to a hundred km.

4) Even when the intensity of the ionospheric contribution amounts to the measurable range, separation of the ionospheric contribution from the background would require some technique, such as multiple correlations and spatial correlations.

As seen in Figs. 4, 5, 7 and 8, the distribution of the ionospheric contribution to the ground electric field is controlled by the spatial extent of the ionospheric electric field, as already noted in Section 2 in relation to the divergence and the convergence of horizontal components. Owing to the sharp decrease in electric conductivity below the ionosphere, even a relatively small pattern, smaller than the 100 km ionospheric height, can penetrate down to the lower atmosphere. This is an important nature of the electric field in contrast to the much more "out of focus" image of the magnetic field produced in the ionosphere when observed on the ground. The electric field on the ground is an image with a higher spatial resolution of the ionospheric electric field than a magnetic field image on the ground reflecting the ionospheric electric currents.

The ground observation of the ionospheric electric field, therefore, requires fine grids of stations at 50 km or smaller, for comparing the spatial distributions of observed electric fields with calculations, and for taking reliable spatial correlations between stations. At the same time, the whole extent of the station network is desirable to cover the whole of auroral activities or the possible extent of the ionospheric electric field in order to determine the distribution pattern. One might wonder if 50 km grid is fine enough to detect the contributions of much smaller auroral patches since it is well known that most pulsating auroral patches are usually smaller than 50 km across. However, as seen in Fig. 5, the contribution decreases remarkably as the size is reduced, and hence it would become undetectable by any means, even if the multiple correlation method is applied. The 50 km, or a little smaller, grids proposed here may be necessary and sufficient to obtain the significant result of the ground measurements of the ionospheric electric fields.

References

OGUTI, T. (1981): TV observations of auroral arcs. Physics of Auroral Arc Formation, ed. by S.-I. AKASOFU and J. R. KAN. Washington, D. C., Am. Geophys. Union, 31–41 (Geophys. Monograph 25).

OGUTI, T. and HAYASHI, K. (1984): Multiple correlation between auroral and magnetic pulsations, 2. Determination of electric currents and electric fields around a pulsating auroral patch. J. Geophys. Res., **89**, 7467–7481.

OGUTI, T., MEEK, J. H. and HAYASHI, K. (1984): Multiple correlation between auroral and magnetic pulsations. J. Geophys. Res., **89**, 2295–2303.

PARK, C. G. (1976): Downward mapping of high latitude ionospheric electric fields to the ground. J. Geophys. Res., **81**, 168–174.

STUBBE, P. and KOPKA, H. (1977): Modulation of the polar electrojet by powerful HF waves. J. Geophys. Res., **82**, 2319–2325.

(Received May 24, 1984; Revised manuscript received October 26, 1984)